

Compatibility of quark and resonant picture excited baryon multiplets in the $1/N_c$ expansion of QCD

Thomas D. Cohen*

Department of Physics, University of Maryland, College Park, Maryland 20742-4111, USA

Richard F. Lebed†

Department of Physics and Astronomy, Arizona State University, Tempe, Arizona 85287-1504, USA

(Received 20 June 2003; published 10 September 2003)

We demonstrate that the two major complementary pictures of large N_c baryon resonances—as single-quark orbital excitations about a closed-shell core [giving $SU(2N_F) \times O(3)$ multiplets], and as resonances in meson-baryon scattering amplitudes—are completely compatible in a specific sense: Both pictures give rise to a set of multiplets of degenerate states, for which any complete spin-flavor multiplet within one picture fills the quantum numbers of complete multiplets in the other picture. This result is demonstrated by (i) straightforward computation of the lowest multiplets in both pictures, (ii) a study of the nature of quark excitations in a hedgehog picture, and (iii) direct group-theoretical comparison of the constraints in the two pictures.

DOI: 10.1103/PhysRevD.68.056003

PACS number(s): 11.15.Pg, 12.39.-x, 13.75.Gx, 14.20.Gk

I. INTRODUCTION

The quark model has historically served as the paradigm for understanding the general patterns of excited baryonic states. In important ways, however, this picture is unsatisfactory. In particular, it is entirely unclear how to obtain the quark model as a direct consequence of fundamental QCD interactions. At a more mundane level, while the quark model describes only bound states of an unchanging number of confined quarks, all of the excited baryons observed in nature appear as resonances in scattering experiments, which are not comprehensible without an understanding of quark production and annihilation dynamics. Thus, in order to compare quark model predictions to experimental data one must make additional *ad hoc* assumptions about the strength and mechanism of such quark processes.

Recently, we argued [1] that large N_c QCD provides insights into both of these issues. In particular, we showed that the “contracted” spin-flavor symmetry [2–5] known to emerge for ground-state baryons directly from large N_c QCD imposes important constraints on the resonance positions (masses and widths) of excited baryons. These constraints imply that various resonances with distinct I and J quantum numbers become degenerate as N_c becomes large. On the other hand, treatments using a large N_c quark picture exhibit precisely the same degeneracy patterns [1,6,7], and thus capture at least some nontrivial QCD dynamics.

Specifically, in Ref. [1] we demonstrated these degeneracies for the case of the mixed-symmetry $\ell=1$ negative-parity states in the simple quark-shell model, where ℓ denotes the orbital angular momentum of a single quark excited with respect to a “core” of N_c-1 quarks symmetrized in spin \times flavor. Explicit diagonalization of the large N_c quark-picture Hamiltonian for these states [8,9] manifests these

mass degeneracies. The purpose of the present paper is to show that the previous result is in fact general and applies to excited states of *any* angular momentum, parity, or symmetry. For simplicity and clarity of presentation, we restrict our attention to the nonstrange sector.

The *operator method* of constructing the baryon Hamiltonian in the large N_c quark-shell picture (i.e., as a linear combination of operators constructed from the spin and flavor degrees of freedom of the individual quark interpolating fields [10]) was originally applied to the ground-state spin-flavor multiplet containing N and Δ [the large N_c analogue to the $SU(6)$ symmetric **56**-plet] [11–14]. References to a number of other applications to the ground-state band are listed in Ref. [15]. Subsequent work extended the method to excited baryons, in particular the $\ell=1$ multiplet [the large N_c analogue of the $SU(6)$ mixed-symmetry **70**-plet] [8,9,16–19], and even higher multiplets [20,21].

On the other hand, the *consistency condition method*, originating directly from the contracted spin-flavor symmetry, tends to be less represented in the literature, even though the method is obtained directly from considerations of meson-baryon scattering processes and thus is closely intertwined with the phenomenon of baryon resonances. The first such work on excited baryons [6] studied resonances by deriving quark-picture operators that satisfy the contracted spin-flavor symmetry, and then used the operators to obtain a Hamiltonian, from which matrix elements describing the spectrum and decays of these states were obtained.

One may, however, question the validity of the operator picture in describing intrinsically unstable systems such as baryon resonances within a Hamiltonian formalism, since the states in the bra and ket of its matrix elements must be assumed to exist for a sufficiently long time in order to be described as eigenstates of a Hamiltonian (rather than simply as bumps in a scattering amplitude). For example, generic large N_c counting shows that meson-baryon scattering amplitudes scale as N_c^0 , suggesting that true baryon resonances have masses above those in the ground-state band [which are

*Electronic address: cohen@physics.umd.edu

†Electronic address: Richard.Lebed@asu.edu

$O(N_c^1)$] by an amount of $O(N_c^0)$, as well as widths that also scale as N_c^0 . On the other hand, Ref. [6] suggests that the $\ell = 1$ excited baryons can have widths of $O(1/N_c)$. Whether there exist baryon resonances exhibiting this property (and therefore rendering them stable in the large N_c limit) remains an open question.

In this paper, however, we adopt the starting point that all baryon resonances arise from generic poles in meson-baryon scattering amplitudes with energies above the ground state of $O(N_c^0)$ and widths of $O(N_c^0)$. Work along these lines [22–26] long predates the operator method papers, and was originally derived not from a quark picture, but from a chiral soliton picture. In the large N_c limit it was shown that the results of this approach may be derived from a simple prescription [24]: In treating the scattering as a t -channel process, the isospin exchanged equals the angular momentum exchanged, the so-called $I_t = J_t$ rule. In Ref. [1], this rule was shown to be equivalent to the scattering consistency conditions derived from the contracted spin-flavor symmetry, which again is a consequence of large N_c without additional model assumptions.

One therefore expects that, if the operator method is physically valid, it must generate a spectrum of states compatible with the resonances obtained from the $I_t = J_t$ rule. It turns out that such resonance multiplets may be labeled by non-negative integers K , which correspond to the “grand spin” of the Skyrme and other chiral soliton models. The “compatibility” of this paper’s title refers to the fact [1] that the spectrum of resonant states obtained in the quark-shell model mixed-symmetry $\ell = 1$ multiplet consists of one member, for each allowed I and J quantum number, from precisely three complete degenerate multiplets (labeled $K = 0, 1$, and 2) in the scattering “resonance” picture. In other words, in that multiplet the (complex) mass parameter for each one of the 13 distinct states equals either $m_{K=0}$, $m_{K=1}$, or $m_{K=2}$. This remarkable correspondence between two very different physical pictures is the motivation for the present work. As suggested above, we show that each (nonstrange) quark-picture multiplet is filled by a collection of resonance-picture K multiplets, one mass (and width) value from each resonance-picture K multiplet appearing for each allowed value of I and J in the quark-picture multiplet.

This paper is arranged as follows: In Sec. II, we discuss in greater detail the resonance picture, the significance of K spin, and linear relations between S -matrix amplitudes. Section III lays out all relevant baryon spin-flavor multiplets for arbitrary N_c , their decomposition into separate spin and flavor multiplets, and relations between quantum numbers of their nonstrange members. In Sec. IV we exhibit explicitly the compatibility of quark-shell and resonance picture states. Section V explains why this compatibility occurs, first using a general description in terms of Skyrme model hedgehog configurations, and second using explicit group-theoretical counting. Discussion and conclusions appear in Sec. VI.

II. MESON-NUCLEON SCATTERING PICTURE

We begin with a brief review of the origin of degeneracies among baryonic resonances. The key to the analysis is the

existence of linear relations among the S matrices of various channels in meson-nucleon scattering (or more generally, scattering of mesons off ground-state band baryons) [22–26]. Here we need only study the scattering of π or η mesons off a ground-state band baryon; these cases are sufficient to connect to all quantum numbers of interest. Note that in the physical world the notion of describing the scattering of unstable mesons such as η off baryons is problematic. However, it is sensible to talk about such scattering in large N_c since these mesons are stable in the large N_c world. The S matrices are related by

$$S_{LL'RR'IJ}^{\pi} = \sum_K (-1)^{R'-R} \sqrt{(2R+1)(2R'+1)(2K+1)} \\ \times \left\{ \begin{matrix} K & I & J \\ R' & L' & 1 \end{matrix} \right\} \left\{ \begin{matrix} K & I & J \\ R & L & 1 \end{matrix} \right\} s_{KL'L}^{\pi}, \\ S_{LRJ}^{\eta} = \sum_K \delta_{KL} \delta(LRJ) s_K^{\eta}. \quad (2.1)$$

The notation is as follows: In the case of π scattering, the incoming baryon spin (which equals its isospin for the nonstrange members of the ground-state band) is denoted as R , final baryon spin (isospin) is denoted R' ; the incident (final) π is in a partial wave of orbital angular momentum L (L'), and I and J represent the (conserved) total isospin and angular momentum, respectively, of the initial and final states. $S_{LL'RR'IJ}^{\pi}$ is the (isospin- and angular-momentum-reduced) S matrix for this channel reduced in the sense of the Wigner-Eckart theorem, the factors in braces are $6j$ coefficients, and $s_{KL'L}^{\pi}$ are universal amplitudes that are independent of I, J, R , and R' . In the case of η scattering, the fact that the meson has $I=0$ more tightly constrains many of the quantum numbers. The isospin (= spin) R of the baryon is unchanged and moreover equals the total isospin I of the intermediate state. The orbital angular momentum L of the η remains unchanged in the process due to the $I_t = J_t$ rule, and J denotes the total angular momentum of the state, which is constrained by the triangle rule $\delta(LRJ)$. S_{LRJ}^{η} is the reduced scattering amplitude and s_K^{η} are universal amplitudes independent of J . The linear relations among the scattering amplitudes can be seen from the structure of Eqs. (2.1). The key point is simply that there are more $S_{LL'RR'IJ}^{\pi}$ amplitudes than there are $s_{KL'L}^{\pi}$ amplitudes. Thus at leading order in $1/N_c$, there are linear constraints between the $S_{LL'RR'IJ}^{\pi}$ amplitudes. There are also more S_{LRJ}^{η} amplitudes than s_K^{η} amplitudes, yielding more nontrivial relations.

Equations (2.1) were first derived in the context of the Skyrme model [22–26]. In this picture, as in other chiral soliton models, the soliton at the classical or mean-field level (which dominates as $N_c \rightarrow \infty$) breaks both the rotational and isospin symmetries but is invariant under $\mathbf{K} \equiv \mathbf{I} + \mathbf{J}$. Accordingly, the intrinsic dynamics of the soliton commutes with the “grand spin” of $\mathbf{I} + \mathbf{J}$, and excitations can be labeled by K . This is the K of Eqs. (2.1). Note that the physical states

are projected from the hedgehogs, so that \mathbf{K} of the physical state is *not* just $\mathbf{I}+\mathbf{J}$, but rather represents the grand spin of the underlying intrinsic state.

The derivation of Eqs. (2.1) from the Skyrme model has the advantage of suggesting a clear physical picture in which the K quantum number has a simple interpretation. Of course, it has the disadvantage of being based on a model rather than directly on large N_c QCD. However, these relations are, in fact, exact results in large N_c QCD and do not depend on any additional model assumptions. A direct derivation based on large N_c consistency rules [5] and exploiting the famous $I_t = J_t$ rule [24] is given in the Appendix of Ref. [1].

Equations (2.1) can be obtained from a more general relation [24]—again equivalent to the $I_t = J_t$ rule—describing meson-baryon scattering of nonstrange particles,

$$m + B \rightarrow m' + B', \quad (2.2)$$

where m (m') is a meson of spin s (s') and isospin i (i'), B (B') is a baryon in the ground-state multiplet with spin = isospin R (R'), and the total spin angular momentum (not including relative orbital angular momentum) of the meson and baryon is denoted S (S'). Adopting the remainder of the symbols from Eqs. (2.1) and abbreviating the multiplicity $2X+1$ of an $SU(2)$ representation of quantum number X by $[X]$, then Eq. (3) of Ref. [24] reads

$$S_{LL'SS'IJ} = \sum_{K, \tilde{K}, \tilde{K}'} [K][R][R'][S][S'][\tilde{K}][\tilde{K}']^{1/2} \times \begin{Bmatrix} L & i & \tilde{K} \\ S & R & s \\ J & I & K \end{Bmatrix} \begin{Bmatrix} L' & i' & \tilde{K}' \\ S' & R' & s' \\ J & I & K \end{Bmatrix} \tau_{K\tilde{K}\tilde{K}'LL'}. \quad (2.3)$$

In the cases considered here, the mesons are both spinless ($s = s' = 0$), which implies the collapse of the $9j$ symbols to $6j$ symbols, and forces $S \rightarrow R$, $S' \rightarrow R'$, and $\tilde{K} = \tilde{K}' = K$. The first of Eqs. (2.1) is then obtained by taking $i = i' = 1$ and $s_{KLL'}^\pi = (-1)^{L-L'} \tau_{KKKLL'}$, while the second of Eqs. (2.1) is obtained by taking $i = i' = 0$ [which further collapses the $6j$ symbols, leaving only $\delta_{LL'} \delta_{RR'} \delta_{IR} \delta(LRJ)$] and by taking $s_K^\eta = \tau_{KKKLL}$.

The pattern of degeneracies of the masses and widths of resonances falls out immediately from the structure of Eqs. (2.1), provided one defines the resonance position to be at the pole. Since resonances are broad, there is some ambiguity in defining precisely what one means by the mass of the resonance. Moreover, since generically baryon resonances in the large N_c limit need not be narrow, these ambiguities can be large. Perhaps the cleanest theoretical way to define the resonance position is via analytic continuation of the scattering amplitude in the complex energy plane (with three-momentum fixed to zero) and to define a resonance as occurring at the point at which the amplitude develops a pole. The resonance mass and width are then the real and imaginary

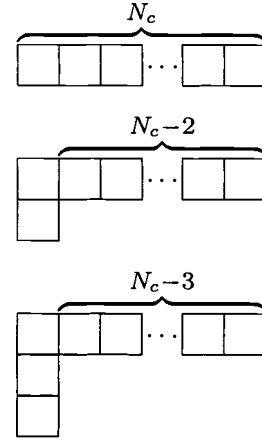


FIG. 1. Young tableaux for the $SU(2N_F)$ S, MS, and A spin-flavor representations, respectively. For $N_F = 3$ these are the familiar **56**, **70**, and **20**, respectively.

parts of the complex pole position. Note that with this definition degeneracies automatically follow. In order for one of the $S_{LL'RR'IJ}^\pi$ amplitudes to diverge, one of the $s_{KL'L}^\pi$ amplitudes must diverge. However, since the $s_{KL'L}^\pi$ amplitudes contribute to multiple channels, all of these channels must have resonances at the same position, which means that the masses and widths of certain resonances in different channels must be degenerate. As seen in Ref. [1], the observed pattern of degeneracies for the low-lying negative-parity $\ell = 1$ baryons obtained for the resonances is identical to that obtained in the large N_c quark-shell picture. Below we show that the coincidence between the pattern of degeneracies for baryon resonances in large N_c QCD and states in the large N_c quark-shell picture holds far more generally.

III. STATES IN THE QUARK-SHELL MODEL PICTURE

The analysis of spin-flavor multiplets in the quark-shell picture is a straightforward, albeit tedious, extension of methods familiar from $N_c = 3$. For $N_c = 3$ only three spin-flavor representations occur: (i) Completely symmetric (S), which is a **56** for $N_F = 3$ or a **20** for $N_F = 2$; (ii) mixed-symmetry (MS), which is a **70** for $N_F = 3$ or a **20** for $N_F = 2$; and (iii) completely antisymmetric (A), which is a **20** for $N_F = 3$ or a **4** for $N_F = 2$. For $N_c > 3$ many other spin-flavor representations are possible, but these do not interest us since they decouple in the physical limit $N_c = 3$. It should be noted that the A representation is only fully antisymmetric for $N_c = 3$, but we maintain the label A for $N_c > 3$. The $N_c > 3$ generalizations of the S, MS, and A representations are presented in Fig. 1. One may assume (as done here) that the additional $(N_c - 3)$ quarks in the lowest-energy multiplets appear in a completely symmetric spin-flavor combination, and examine whether this ansatz gives a phenomenologically viable $1/N_c$ expansion. Alternately, although baryon spin-flavor representations with more than one pair of antisymmetrized indices exist for $N_c > 3$, such states do not exist in the physical $N_c = 3$ universe and are thus ignored in the following analysis.

The first step in the analysis is to decompose $SU(2N_F)$

spin \times flavor representations into separate SU(2) spin and SU(N_F) flavor representations. This is a fairly straightforward but tedious exercise in pairing spin and flavor representations with the correct overall spin-flavor transformation properties. To illustrate the results, we employ the SU(N_F) Dynkin label, which is an $(N_F - 1)$ -plet $[n_1, n_2, \dots, n_{N_F-1}]$ of non-negative integers n_r describing the Young diagram of

the representation: The number of boxes in row r of the Young diagram exceeds the number in row $r+1$ by n_r . In this notation, the S multiplet is $[N_c, 0, 0, \dots, 0]$, MS is $[N_c - 2, 1, 0, 0, \dots, 0]$, and A is $[N_c - 3, 0, 1, 0, 0, \dots, 0]$. SU(2) spin representations can also be represented in this way, but it is more convenient to use the quantum number S as a label.

One then finds the (flavor, S) representations

$$S \equiv [N_c, 0, 0, \dots, 0] = \bigoplus_{n=0}^{(N_c-1)/2} \left(\left[2n+1, \frac{1}{2}(N_c-1)-n, 0, 0, \dots, 0 \right], n + \frac{1}{2} \right), \quad (3.1)$$

$$\begin{aligned} MS \equiv [N_c - 2, 1, 0, 0, \dots, 0] = & \bigoplus_{n=0}^{(N_c-5)/2} \left(\left[2n+2, \frac{1}{2}(N_c-5)-n, 1, 0, 0, \dots, 0 \right], n + \frac{1}{2} \right) \\ & \bigoplus_{n=0}^{(N_c-3)/2} \left(\left[2n, \frac{1}{2}(N_c-3)-n, 1, 0, 0, \dots, 0 \right], n + \frac{1}{2} \right) \\ & \bigoplus_{n=0}^{(N_c-3)/2} \left(\left[2n+1, \frac{1}{2}(N_c-1)-n, 0, 0, \dots, 0 \right], n + \frac{3}{2} \right) \\ & \bigoplus_{n=0}^{(N_c-3)/2} \left(\left[2n+1, \frac{1}{2}(N_c-1)-n, 0, 0, \dots, 0 \right], n + \frac{1}{2} \right) \\ & \bigoplus_{n=0}^{(N_c-3)/2} \left(\left[2n+3, \frac{1}{2}(N_c-3)-n, 0, 0, \dots, 0 \right], n + \frac{1}{2} \right), \end{aligned} \quad (3.2)$$

$$\begin{aligned} A \equiv [N_c - 3, 0, 1, 0, 0, \dots, 0] = & \bigoplus_{n=0}^{(N_c-5)/2} \left(\left[2n+1, \frac{1}{2}(N_c-5)-n, 0, 1, 0, 0, \dots, 0 \right], n + \frac{3}{2} \right) \\ & \bigoplus_{n=0}^{(N_c-5)/2} \left(\left[2n+1, \frac{1}{2}(N_c-5)-n, 0, 1, 0, 0, \dots, 0 \right], n + \frac{1}{2} \right) \\ & \bigoplus_{n=0}^{(N_c-7)/2} \left(\left[2n+3, \frac{1}{2}(N_c-7)-n, 0, 1, 0, 0, \dots, 0 \right], n + \frac{1}{2} \right) \\ & \bigoplus_{n=0}^{(N_c-5)/2} \left(\left[2n+2, \frac{1}{2}(N_c-5)-n, 1, 0, 0, \dots, 0 \right], n + \frac{3}{2} \right) \\ & 2 \bigoplus_{n=0}^{(N_c-5)/2} \left(\left[2n+2, \frac{1}{2}(N_c-5)-n, 1, 0, 0, \dots, 0 \right], n + \frac{1}{2} \right) \\ & \bigoplus_{n=0}^{(N_c-5)/2} \left(\left[2n, \frac{1}{2}(N_c-3)-n, 1, 0, 0, \dots, 0 \right], n + \frac{1}{2} \right) \\ & \bigoplus_{n=0}^{(N_c-7)/2} \left(\left[2n+4, \frac{1}{2}(N_c-7)-n, 1, 0, 0, \dots, 0 \right], n + \frac{1}{2} \right) \\ & \bigoplus_{n=0}^{(N_c-7)/2} \left(\left[2n+1, \frac{1}{2}(N_c-7)-n, 2, 0, 0, \dots, 0 \right], n + \frac{1}{2} \right) \end{aligned}$$

$$\begin{aligned}
& \bigoplus_{n=0}^{(N_c-5)/2} \left[\left[2n+1, \frac{1}{2}(N_c-1)-n, 0, 0, \dots, 0 \right], n+\frac{3}{2} \right) \\
& \bigoplus_{n=0}^{(N_c-5)/2} \left[\left[2n+3, \frac{1}{2}(N_c-3)-n, 0, 0, \dots, 0 \right], n+\frac{1}{2} \right) \\
& \bigoplus_{n=0}^{(N_c-3)/2} \left[\left[2n, \frac{1}{2}(N_c-3)-n, 1, 0, 0, \dots, 0 \right], n+\frac{3}{2} \right) \\
& \bigoplus_{n=0}^{(N_c-3)/2} \left[\left[2n+1, \frac{1}{2}(N_c-1)-n, 0, 0, \dots, 0 \right], n+\frac{1}{2} \right). \tag{3.3}
\end{aligned}$$

For example, in the $N_F=3$, $N_c=3$ case [the familiar $SU(6) \rightarrow SU(3) \times SU(2)$ decomposition], any sum with an upper limit smaller than $(N_c-3)/2$ vanishes, as does any multiplet with a nonzero value in the fourth (or higher) entry of a flavor multiplet Dynkin symbol, since this would require four quark flavors among which to antisymmetrize. All that remains in this case is the $n=0$ and 1 members of $S=56$, which are $(8, 1/2)$ and $(10, 3/2)$, respectively; the $n=0$ member of each of the last four sums in $MS=70$, which are $(1, 1/2)$, $(8, 3/2)$, $(8, 1/2)$, and $(10, 1/2)$, respectively; and the $n=0$ member of each of the last two sums in $A=20$, which are $(1, 3/2)$ and $(8, 1/2)$, respectively.

More generally, we are interested only in those states with quantum numbers that appear for $N_c=3$, in particular $I=1/2$ or $3/2$, since isospin is a good quantum number for any N_c . Furthermore, in this work we consider for simplicity only the nonstrange states; the strange states are more difficult only for technical group-theoretical reasons, and are deferred to future work [27].

These restrictions dramatically simplify the list of multiplets that must be considered. The tallest column of the Young diagram (with a number of boxes equal to the *position* of the last nonzero entry of the Dynkin label) indicates the number of distinct quark flavors that must be present for each state of the multiplet for the diagram to be allowed. For our purposes, then, one may discard any multiplet with a nonzero entry in n_3 , n_4 , etc., and consider only Young diagrams with at most two rows. The first entry of the Dynkin label n_1 then indicates the maximum number of quarks of one flavor (u , d , etc.) that may be symmetrized in any state of the multiplet, and the second entry indicates the number of quark pairs antisymmetrized in flavor. Since the nonstrange states, lying in the top row of the weight diagram, are singly degenerate, the isospin I of the multiplet equals the maximum allowed I_3 value; this, in turn, is just $\frac{1}{2}n_1$. Thus, only $n_1 \leq 3$ need be included.

The multiplets of interest, using the notation I_S and the shorthand $I=\frac{1}{2} \rightarrow N$, $I=\frac{3}{2} \rightarrow \Delta$, then read

$$S: N_{1/2} \oplus \Delta_{3/2}, \tag{3.4}$$

$$MS: N_{1/2} \oplus N_{3/2} \oplus \overbrace{\Delta_{1/2} \oplus \Delta_{3/2} \oplus \Delta_{5/2}}^{N_c \geq 5}, \tag{3.5}$$

$$A: \overbrace{N_{1/2} \oplus N_{3/2} \oplus \Delta_{1/2} \oplus \Delta_{3/2}}^{N_c \geq 5} \oplus \overbrace{\Delta_{5/2}}^{N_c \geq 7}. \tag{3.6}$$

It is interesting to note that the A representation is, for large N_c , much larger than the MS representation; however, for any $N_c \geq 7$ they contain exactly the same nonstrange $I=\frac{1}{2}$ and $\frac{3}{2}$ states (a fact to be explained in Sec. V). Yet, even for the nonstrange states the MS and A multiplets differ for the highest values of isospin: By comparing Eqs. (3.2) and (3.3), one finds MS contains states $(I, S) = (N_c/2-1, N_c/2)$ and $(N_c/2, N_c/2-1)$ that A does not.

Another interesting fact, to be used later, is that the N and Δ states in the MS or A representations in Eqs. (3.4)–(3.6) (before excited quark angular momentum ℓ is added) have the curious property that their total quark spins S are precisely those obtained from vectorially adding one unit of angular momentum to the S values of the N, Δ in the S representation before ℓ is added [Eq. (3.4)]; this fact was noted in Ref. [6]. We shall see why this occurs in Sec. V. Let us label this effective angular momentum Δ , so that each value of $S_{MS/A}$ satisfying $\delta(S_S, S_{MS/A}, \Delta=1)$ occurs. Then, since the multiplets for $\ell \neq 0$ (given in Table I) are obtained through the vector addition $\mathbf{J}=\mathbf{S}+\boldsymbol{\ell}$, and since the same total angular momentum quantum numbers are obtained through any order of vector addition, it follows that the $\ell \neq 0$ MS/A J eigenvalues may be obtained through vector addition of Δ to those of S. Thus, each value of $J_{MS/A}$ satisfying $\delta(J_S, J_{MS/A}, \Delta=1)$ occurs, with the same multiplicity as given by the vector addition

$$\begin{aligned}
\mathbf{J}_{MS/A} &= \mathbf{S}_{MS/A} + \boldsymbol{\ell}_{MS/A} \\
&= \mathbf{J}_S + \boldsymbol{\Delta} \quad (\text{effectively}) \\
&= \mathbf{S}_S + \boldsymbol{\ell}_S + \boldsymbol{\Delta} \equiv \mathbf{S}_S + \boldsymbol{\ell}_{\text{eff}}. \tag{3.7}
\end{aligned}$$

TABLE I. Nonstrange states of $I = \frac{1}{2}$ and $\frac{3}{2}$ in the large N_c S, MS, and MA spin-flavor representations and various values of the excited quark orbital angular momentum ℓ .

Representation	ℓ	States
S	0	$N_{1/2} \oplus \Delta_{3/2}$
	1	$N_{1/2} \oplus N_{3/2} \oplus \Delta_{1/2} \oplus \Delta_{3/2} \oplus \Delta_{5/2}$
	2	$N_{3/2} \oplus N_{5/2} \oplus \Delta_{1/2} \oplus \Delta_{3/2} \oplus \Delta_{5/2} \oplus \Delta_{7/2}$
	3	$N_{5/2} \oplus N_{7/2} \oplus \Delta_{3/2} \oplus \Delta_{5/2} \oplus \Delta_{7/2} \oplus \Delta_{9/2}$
MS or A	0	$N_{1/2} \oplus N_{3/2} \oplus \Delta_{1/2} \oplus \Delta_{3/2} \oplus \Delta_{5/2}$
	1	$2N_{1/2} \oplus 2N_{3/2} \oplus N_{5/2} \oplus 2\Delta_{1/2} \oplus 3\Delta_{3/2} \oplus 2\Delta_{5/2} \oplus \Delta_{7/2}$
	2	$N_{1/2} \oplus 2N_{3/2} \oplus 2N_{5/2} \oplus N_{7/2} \oplus 2\Delta_{1/2} \oplus 3\Delta_{3/2} \oplus 3\Delta_{5/2} \oplus 2\Delta_{7/2} \oplus \Delta_{9/2}$
	3	$N_{3/2} \oplus 2N_{5/2} \oplus 2N_{7/2} \oplus N_{9/2} \oplus \Delta_{1/2} \oplus 2\Delta_{3/2} \oplus 3\Delta_{5/2} \oplus 3\Delta_{7/2} \oplus 2\Delta_{9/2} \oplus \Delta_{11/2}$

This implies that the MS/A states of a given ℓ occur with the same quantum numbers and multiplicities as appear in an effective collection of S multiplets, each with its own value ℓ_{eff} that assumes all values satisfying $\delta(\ell_{\text{eff}}, \ell, \Delta = 1)$.

What remains is to add an orbital angular momentum ℓ to the total quark spin S in order to obtain the total spin J of the state. For the conventional states in which all quarks have positive parity, the overall parity of the baryon is that contributed by the orbital excitation, $P = (-1)^\ell$. However, we shall see that all of our results are blind to P (except that it must be conserved in strong interactions), and thus one may classify quark-picture states in Table I by their $\text{SU}(2N_F) \times \text{O}(3)$ representation without the need of specifying P .

IV. COMPATIBILITY

The multiplicities of quark-picture states in Table I may be compared immediately with those in the meson-nucleon scattering results presented in Tables II and III, which in turn are obtained via Eqs. (2.1). Simply note first that the K amplitudes appearing for a resonance of given spin and flavor quantum numbers (e.g., $\Delta_{1/2}$) are the same regardless of the parity P : The $I_t = J_t$ rule makes no reference to P . Of course, one should not expect the poles for K amplitudes with $+$ and $-$ parities to be equal, hence the tilde on each mass in the $P = +$ case. Nevertheless, this “parity blindness” mirrors that found in the $\text{SU}(2N_F) \times \text{O}(3)$ multiplets in the quark picture.

The principal result of this work is illustrated by the fact that the quark-picture multiplet structures listed in Table I are found to be completely compatible with those listed in Tables II and III. To be precise, for all values $\ell = 0, 1, 2, 3$, one sees that an S multiplet of given ℓ contains only a single mass eigenvalue m_ℓ , degenerate among all states in the multiplet up to and including effects of $\text{O}(N_c^0)$, the order of meson-baryon scattering. This mass eigenvalue is seen to occur for, and only for, states that can accommodate a K amplitude with $K = \ell$. Furthermore, a MS or an A multiplet of given ℓ contains precisely those mass eigenvalues m_K such that K assumes all values satisfying the triangle rule $\delta(K\ell 1)$.

Thus, for example, each state in the MS $\ell = 2$ multiplet in Table I assumes one of three possible mass eigenvalues degenerate to $\text{O}(N_c^0)$: m_1 , m_2 , or m_3 . On the other hand, one can see by referring to Tables II and III that all states given in the next-to-last line of Table I appear as poles with $K = 1, 2$, or 3 , with precisely the right multiplicities as predicted by Tables II and III. Thus only a single MS $\ell = 2$ $N_{1/2}$ state occurs, despite the fact that Tables II and III allow for two poles with $N_{1/2}$ quantum numbers (m_0 and m_1), simply because the m_0 pole (from a $K = 0$ amplitude) does not appear in the MS $\ell = 2$ multiplet. On the other hand, the quark-picture multiplet contains no $N_{9/2}$ state, while the scattering amplitudes with $N_{9/2}$ quantum numbers contain no contribution $K = 1, 2$, or 3 , and hence no m_1 , m_2 , or m_3 pole.

We hasten to add two comments. The first is that we have demonstrated only the *compatibility* of quark-picture $\text{SU}(2N_F) \times \text{O}(3)$ and meson-baryon scattering-picture degeneracies among baryon resonances; we have not proved that the two pictures are the same, but rather only that they can be assumed simultaneously correct in their descriptions of the multiplet patterns without contradictions or the necessity of imposing strong constraints on any configuration mixing between multiplets. Indeed, no explicit proof of statements regarding the degeneracy of mass eigenvalues in the quark-shell picture has been given thus far (except for previous results for the symmetric $\ell = 0$ ground-state multiplet [4,5,11], the MS $\ell = 1$ excited multiplet [8], and the S $\ell = 2$ multiplet [21]), but a general argument (using a hedgehog-based analysis) appears in Sec. V. Second, we have carried out this demonstration explicitly only up to $\ell = 3$. While one might suspect that the chances of the result not being generic is exceedingly small, it is still of great value to see a general proof, as well as to understand the underlying symmetry reason for this remarkable compatibility.

V. A GENERAL DEMONSTRATION

The previous three sections provide a rather circuitous demonstration of what appears to be a simple result: Namely, the spectrum of states for *any* $\text{SU}(4) \times \text{O}(3)$ multiplet (of either P) consists of a small set of eigenvalues $\{m_K\}$. Here, K refers to K -spin value of the meson-baryon (reduced) scattering amplitudes that can accommodate the I, J quantum numbers of states in the multiplet possessing the particular eigenvalue m_K . Therefore, m_K gives the position of a (complex) pole in an amplitude with this K -spin value. On the other hand, scattering amplitudes with given I, J quantum numbers do *not* contain amplitudes of a particular K , and hence have no pole at m_K , *unless* a state with these I, J values appears in an $\text{SU}(4) \times \text{O}(3)$ multiplet possessing m_K as one of its mass eigenvalues.

In review, there are two basic pictures for baryon resonances: (i) the $\text{SU}(4) \times \text{O}(3)$ classification derived from the quark-shell picture of orbital single-quark excitations about a spin-flavor symmetric core (the *quark* or *operator* picture), and (ii) the meson-baryon scattering classification derived from symmetry features shared by all chiral soliton models (the *resonance* or *scattering* picture). *We now show that the*

TABLE II. Negative-parity mass eigenvalues in the quark-shell model picture, corresponding partial waves, and their expansions in terms of K amplitudes. The superscripts πNN , $\pi N\Delta$, $\pi\Delta\Delta$, ηNN , and $\eta\Delta\Delta$ refer to the scattered meson and the initial and final baryons, respectively. The partial-wave amplitudes are derived from Eqs. (2.1). Note that these states are those appropriate to a large N_c world (as discussed in the text, some do not occur for $N_c=3$). We only list states with total isospin $3/2$ or less, and diagonal in the scattered meson and orbital angular momentum ($L=L'$).

State	Masses accommodated	Partial wave, K amplitudes
$N_{1/2}$	m_0, m_1	$S_{11}^{\pi NN} = s_{100}^{\pi}$ $S_{11}^{\eta NN} = s_0^{\eta}$ $D_{11}^{\pi\Delta\Delta} = s_{122}^{\pi}$
$\Delta_{1/2}$	m_1, m_2	$S_{31}^{\pi NN} = s_{100}^{\pi}$ $D_{31}^{\pi\Delta\Delta} = \frac{1}{10}(s_{122}^{\pi} + 9s_{222}^{\pi})$ $D_{31}^{\eta\Delta\Delta} = s_2^{\eta}$
$N_{3/2}$	m_1, m_2	$S_{13}^{\pi\Delta\Delta} = s_{100}^{\pi}$ $D_{13}^{\pi NN} = \frac{1}{2}(s_{122}^{\pi} + s_{222}^{\pi})$ $D_{13}^{\pi N\Delta} = \frac{1}{2}(s_{122}^{\pi} - s_{222}^{\pi})$ $D_{13}^{\pi\Delta\Delta} = \frac{1}{2}(s_{122}^{\pi} + s_{222}^{\pi})$ $D_{13}^{\eta NN} = s_2^{\eta}$
$\Delta_{3/2}$	m_0, m_1, m_2, m_3	$S_{33}^{\pi\Delta\Delta} = s_{100}^{\pi}$ $S_{33}^{\eta\Delta\Delta} = s_0^{\eta}$ $D_{33}^{\pi NN} = \frac{1}{20}(s_{122}^{\pi} + 5s_{222}^{\pi} + 14s_{322}^{\pi})$ $D_{33}^{\pi N\Delta} = \frac{1}{5\sqrt{10}}(2s_{122}^{\pi} + 5s_{222}^{\pi} - 7s_{322}^{\pi})$ $D_{33}^{\pi\Delta\Delta} = \frac{1}{25}(8s_{122}^{\pi} + 10s_{222}^{\pi} + 7s_{322}^{\pi})$ $D_{33}^{\eta\Delta\Delta} = s_2^{\eta}$
$N_{5/2}$	m_2, m_3	$D_{15}^{\pi NN} = \frac{1}{9}(2s_{222}^{\pi} + 7s_{322}^{\pi})$ $D_{15}^{\pi N\Delta} = \frac{\sqrt{14}}{9}(s_{222}^{\pi} - s_{322}^{\pi})$ $D_{15}^{\pi\Delta\Delta} = \frac{1}{9}(7s_{222}^{\pi} + 2s_{322}^{\pi})$ $D_{15}^{\eta NN} = s_2^{\eta}$ $G_{15}^{\pi\Delta\Delta} = s_{344}^{\pi}$
$\Delta_{5/2}$	m_1, m_2, m_3, m_4	$D_{35}^{\pi NN} = \frac{1}{90}(27s_{122}^{\pi} + 35s_{222}^{\pi} + 28s_{322}^{\pi})$ $D_{35}^{\pi N\Delta} = \frac{1}{90}\sqrt{\frac{7}{5}}(27s_{122}^{\pi} + 5s_{222}^{\pi} - 32s_{322}^{\pi})$ $D_{35}^{\pi\Delta\Delta} = \frac{1}{450}(189s_{122}^{\pi} + 5s_{222}^{\pi} + 256s_{322}^{\pi})$ $D_{35}^{\eta\Delta\Delta} = s_2^{\eta}$ $G_{35}^{\pi\Delta\Delta} = \frac{1}{4}(s_{344}^{\pi} + 3s_{444}^{\pi})$ $G_{35}^{\eta\Delta\Delta} = s_4^{\eta}$

TABLE II. (*Continued*).

State	Masses accommodated	Partial wave, K amplitudes
$N_{7/2}$	m_3, m_4	$D_{17}^{\pi\Delta\Delta} = s_{322}^{\pi}$ $G_{17}^{\pi NN} = \frac{1}{12}(7s_{344}^{\pi} + 5s_{444}^{\pi})$ $G_{17}^{\pi N\Delta} = \frac{\sqrt{35}}{12}(s_{344}^{\pi} - s_{444}^{\pi})$ $G_{17}^{\pi\Delta\Delta} = \frac{1}{12}(5s_{344}^{\pi} + 7s_{444}^{\pi})$ $G_{17}^{\eta NN} = s_4^{\eta}$
$\Delta_{7/2}$	m_2, m_3, m_4, m_5	$D_{37}^{\pi\Delta\Delta} = \frac{1}{5}(2s_{222}^{\pi} + 3s_{322}^{\pi})$ $D_{37}^{\eta\Delta\Delta} = s_2^{\eta}$ $G_{37}^{\pi NN} = \frac{1}{72}(35s_{344}^{\pi} + 33s_{444}^{\pi} + 22s_{544}^{\pi})$ $G_{37}^{\pi N\Delta} = \frac{1}{45}\sqrt{\frac{7}{2}}(5s_{344}^{\pi} + 6s_{444}^{\pi} - 11s_{544}^{\pi})$ $G_{37}^{\pi\Delta\Delta} = \frac{1}{225}(100s_{344}^{\pi} + 48s_{444}^{\pi} + 77s_{544}^{\pi})$ $G_{37}^{\eta\Delta\Delta} = s_4^{\eta}$
$N_{9/2}$	m_4, m_5	$G_{19}^{\pi NN} = \frac{1}{15}(4s_{444}^{\pi} + 11s_{544}^{\pi})$ $G_{19}^{\pi N\Delta} = \frac{2}{15}\sqrt{11}(s_{444}^{\pi} - s_{544}^{\pi})$ $G_{19}^{\pi\Delta\Delta} = \frac{1}{15}(11s_{444}^{\pi} + 4s_{544}^{\pi})$ $G_{19}^{\eta NN} = s_4^{\eta}$ $I_{19}^{\pi\Delta\Delta} = s_{566}^{\pi}$
$\Delta_{9/2}$	m_3, m_4, m_5, m_6	$G_{39}^{\pi NN} = \frac{1}{90}(35s_{344}^{\pi} + 33s_{444}^{\pi} + 22s_{544}^{\pi})$ $G_{39}^{\pi N\Delta} = \frac{1}{90}\sqrt{\frac{11}{10}}(35s_{344}^{\pi} - 3s_{444}^{\pi} - 32s_{544}^{\pi})$ $G_{39}^{\pi\Delta\Delta} = \frac{1}{900}(385s_{344}^{\pi} + 3s_{444}^{\pi} + 512s_{544}^{\pi})$ $G_{39}^{\eta\Delta\Delta} = s_4^{\eta}$ $I_{39}^{\pi\Delta\Delta} = \frac{1}{10}(3s_{566}^{\pi} + 7s_{666}^{\pi})$ $I_{39}^{\eta\Delta\Delta} = s_6^{\eta}$
$\Delta_{11/2}$	m_4, m_5, m_6, m_7	$G_{3,11}^{\pi\Delta\Delta} = \frac{1}{25}(12s_{444}^{\pi} + 13s_{544}^{\pi})$ $G_{3,11}^{\eta\Delta\Delta} = s_4^{\eta}$ $I_{3,11}^{\pi NN} = \frac{1}{468}(55s_{566}^{\pi} + 143s_{666}^{\pi} + 270s_{766}^{\pi})$ $I_{3,11}^{\pi N\Delta} = \frac{1}{117}\sqrt{\frac{55}{14}}(14s_{566}^{\pi} + 13s_{666}^{\pi} - 27s_{766}^{\pi})$ $I_{3,11}^{\pi\Delta\Delta} = \frac{1}{819}(392s_{566}^{\pi} + 130s_{666}^{\pi} + 297s_{766}^{\pi})$ $I_{3,11}^{\eta\Delta\Delta} = s_6^{\eta}$

underlying reason for the compatibility of the two pictures is simply that they obey essentially the same symmetry constraints.

Two different routes lead to this general result. To see them, consider the derivation of Eqs. (2.1), or more generally Eq. (2.3), to describe the symmetry constraints on meson-

baryon scattering. These relations were first obtained in the context of the Skyrme model [22–26]. In this picture, the quantum number K has a simple physical interpretation: The Skyrmion is a chiral soliton at the classical or mean-field level, which at leading order in large N_c has a hedgehog structure. Thus it breaks both the rotational and isospin sym-

TABLE III. The positive-parity amplitudes. The notation is as in Table II.

State	Masses accommodated	Partial wave, K amplitudes
$N_{1/2}$	\tilde{m}_0, \tilde{m}_1	$P_{11}^{\pi NN} = \frac{1}{3}(s_{011}^\pi + 2s_{111}^\pi)$ $P_{11}^{\pi N\Delta} = \frac{\sqrt{2}}{3}(s_{011}^\pi - s_{111}^\pi)$ $P_{11}^{\pi\Delta\Delta} = \frac{1}{3}(2s_{011}^\pi + s_{111}^\pi)$ $P_{11}^{\eta NN} = s_1^\eta$
$\Delta_{1/2}$	\tilde{m}_1, \tilde{m}_2	$P_{31}^{\pi NN} = \frac{1}{6}(s_{111}^\pi + 5s_{211}^\pi)$ $P_{31}^{\pi N\Delta} = \frac{\sqrt{5}}{6}(s_{111}^\pi - s_{211}^\pi)$ $P_{31}^{\pi\Delta\Delta} = \frac{1}{6}(5s_{111}^\pi + s_{211}^\pi)$ $P_{31}^{\eta\Delta\Delta} = s_1^\eta$
$N_{3/2}$	\tilde{m}_1, \tilde{m}_2	$P_{13}^{\pi NN} = \frac{1}{6}(s_{111}^\pi + 5s_{211}^\pi)$ $P_{13}^{\pi N\Delta} = \frac{\sqrt{5}}{6}(s_{111}^\pi - s_{211}^\pi)$ $P_{13}^{\pi\Delta\Delta} = \frac{1}{6}(5s_{111}^\pi + s_{211}^\pi)$ $P_{13}^{\eta NN} = s_1^\eta$ $F_{13}^{\pi\Delta\Delta} = s_{233}^\pi$
$\Delta_{3/2}$	$\tilde{m}_0, \tilde{m}_1, \tilde{m}_2, \tilde{m}_3$	$P_{33}^{\pi NN} = \frac{1}{12}(2s_{011}^\pi + 5s_{111}^\pi + 5s_{211}^\pi)$ $P_{33}^{\pi N\Delta} = \frac{1}{\sqrt{2}}(s_{011}^\pi + s_{111}^\pi - 2s_{211}^\pi)$ $P_{33}^{\pi\Delta\Delta} = \frac{1}{15}(5s_{011}^\pi + 2s_{111}^\pi + 8s_{211}^\pi)$ $P_{33}^{\eta\Delta\Delta} = s_1^\eta$ $F_{33}^{\pi\Delta\Delta} = \frac{1}{5}(s_{233}^\pi + 4s_{333}^\pi)$ $F_{33}^{\eta\Delta\Delta} = s_3^\eta$
$N_{5/2}$	\tilde{m}_2, \tilde{m}_3	$P_{15}^{\pi\Delta\Delta} = s_{211}^\pi$ $F_{15}^{\pi NN} = \frac{1}{9}(5s_{233}^\pi + 4s_{333}^\pi)$ $F_{15}^{\pi N\Delta} = \frac{2}{9}\sqrt{5}(s_{233}^\pi - s_{333}^\pi)$ $F_{15}^{\pi\Delta\Delta} = \frac{1}{9}(4s_{233}^\pi + 5s_{333}^\pi)$ $F_{15}^{\eta NN} = s_3^\eta$
$\Delta_{5/2}$	$\tilde{m}_1, \tilde{m}_2, \tilde{m}_3, \tilde{m}_4$	$P_{35}^{\pi\Delta\Delta} = \frac{1}{19}(3s_{111}^\pi + 7s_{211}^\pi)$ $P_{35}^{\eta\Delta\Delta} = s_1^\eta$ $F_{35}^{\pi NN} = \frac{1}{126}(10s_{233}^\pi + 35s_{333}^\pi + 81s_{433}^\pi)$ $F_{35}^{\pi N\Delta} = \frac{1}{126\sqrt{2}}(32s_{233}^\pi + 49s_{333}^\pi - 81s_{433}^\pi)$ $F_{35}^{\pi\Delta\Delta} = \frac{1}{1260}(512s_{233}^\pi + 343s_{333}^\pi + 405s_{433}^\pi)$ $F_{35}^{\eta\Delta\Delta} = s_3^\eta$

TABLE III. (*Continued*).

State	Masses accommodated	Partial wave, K amplitudes
$N_{7/2}$	\tilde{m}_3, \tilde{m}_4	$F_{17}^{\pi NN} = \frac{1}{4}(s_{333}^{\pi} + 3s_{433}^{\pi})$ $F_{17}^{\pi N\Delta} = \frac{\sqrt{3}}{4}(s_{333}^{\pi} - s_{433}^{\pi})$ $F_{17}^{\pi\Delta\Delta} = \frac{3}{4}(3s_{333}^{\pi} + s_{433}^{\pi})$ $F_{17}^{\eta NN} = s_3^{\eta}$ $H_{17}^{\pi\Delta\Delta} = s_{455}^{\pi}$
$\Delta_{7/2}$	$\tilde{m}_2, \tilde{m}_3, \tilde{m}_4, \tilde{m}_5$	$F_{37}^{\pi NN} = \frac{1}{56}(20s_{233}^{\pi} + 21s_{333}^{\pi} + 15s_{433}^{\pi})$ $F_{37}^{\pi N\Delta} = \frac{1}{7}\sqrt{\frac{15}{2}}(s_{233}^{\pi} - s_{433}^{\pi})$ $F_{37}^{\pi\Delta\Delta} = \frac{1}{7}(3s_{233}^{\pi} + 4s_{433}^{\pi})$ $F_{37}^{\eta\Delta\Delta} = s_3^{\eta}$ $H_{37}^{\pi\Delta\Delta} = \frac{1}{25}(7s_{455}^{\pi} + 18s_{555}^{\pi})$ $H_{37}^{\eta\Delta\Delta} = s_5^{\eta}$
$N_{9/2}$	\tilde{m}_4, \tilde{m}_5	$F_{19}^{\pi\Delta\Delta} = s_{433}^{\pi}$ $H_{19}^{\pi NN} = \frac{1}{5}(3s_{455}^{\pi} + 2s_{555}^{\pi})$ $H_{19}^{\pi N\Delta} = \frac{\sqrt{6}}{5}(s_{455}^{\pi} - s_{555}^{\pi})$ $H_{19}^{\pi\Delta\Delta} = \frac{1}{5}(2s_{455}^{\pi} + 3s_{555}^{\pi})$ $H_{19}^{\eta\Delta\Delta} = s_5^{\eta}$
$\Delta_{9/2}$	$\tilde{m}_3, \tilde{m}_4, \tilde{m}_5, \tilde{m}_6$	$F_{39}^{\pi\Delta\Delta} = \frac{1}{20}(9s_{333}^{\pi} + 11s_{433}^{\pi})$ $F_{19}^{\eta\Delta\Delta} = s_3^{\eta}$ $H_{39}^{\pi NN} = \frac{1}{110}(12s_{455}^{\pi} + 33s_{555}^{\pi} + 65s_{655}^{\pi})$ $H_{39}^{\pi N\Delta} = \frac{1}{110}\sqrt{\frac{3}{5}}(32s_{455}^{\pi} + 33s_{555}^{\pi} - 65s_{655}^{\pi})$ $H_{39}^{\pi\Delta\Delta} = \frac{1}{550}(256s_{455}^{\pi} + 99s_{555}^{\pi} + 195s_{655}^{\pi})$ $H_{39}^{\eta\Delta\Delta} = s_5^{\eta}$
$\Delta_{11/2}$	$\tilde{m}_4, \tilde{m}_5, \tilde{m}_6, \tilde{m}_7$	$H_{3,11}^{\pi NN} = \frac{1}{396}(162s_{455}^{\pi} + 143s_{555}^{\pi} + 91s_{655}^{\pi})$ $H_{3,11}^{\pi N\Delta} = \frac{1}{495}\sqrt{\frac{13}{2}}(81s_{455}^{\pi} - 11s_{555}^{\pi} - 70s_{655}^{\pi})$ $H_{3,11}^{\pi\Delta\Delta} = \frac{1}{2475}(1053s_{455}^{\pi} + 22s_{555}^{\pi} + 1400s_{655}^{\pi})$ $H_{3,11}^{\eta\Delta\Delta} = s_5^{\eta}$ $K_{3,11}^{\pi\Delta\Delta} = \frac{1}{35}(11s_{677}^{\pi} + 24s_{777}^{\pi})$ $K_{3,11}^{\eta\Delta\Delta} = s_7^{\eta}$

metries separately, but does not break the grand spin K defined by $\mathbf{K} \equiv \mathbf{I} + \mathbf{J}$. The soliton's intrinsic dynamics (that not associated with collective zero modes) is governed by a Hamiltonian that commutes with K , so that excitations and scattering states can be labeled by K . The full relations fol-

low from projecting such states, consisting of an excitation characterized by K on top of the hedgehog, onto channels of good I and J .

An alternative, more formal, derivation of these results is given in the Appendix of Ref. [1]. One uses the fact that

matrix elements in baryon states are fixed by the contracted $SU(2N_F)$ spin-flavor symmetry, which in turn requires that, in order to contribute at leading order in $1/N_c$, the operator must have $I=J$. Writing the meson-baryon scattering amplitude as a matrix element of a scattering operator in a space of asymptotic baryon + meson states, one sees that this operator implies $I_t=J_t$, where t indicates the angular momentum and isospin exchanged in the t channel. Using standard group-theoretical identities to cross from the t channel to the s channel gives the relations (2.3). The K quantum number then emerges as a summation variable in an identity involving $6j$ coefficients, and labels the fundamental underlying scattering amplitudes, independent of I or J .

In a similar way we can understand the compatibility discussed above in terms of either a simple physical picture involving excitations of hedgehogs, or in terms of a more formal group-theoretical treatment. We include both treatments here.

A. Physical (hedgehog) demonstration

We begin with the hedgehog-based analysis. The proof exploits some simple operator relations. Assume a Hamiltonian \hat{H} possessing an eigenstate $|\psi_a\rangle$ with eigenvalue E_a . Furthermore, assume an operator $\hat{\Lambda}$ with the property

$$[\hat{H}, \hat{\Lambda}] = \lambda \hat{\Lambda}. \quad (5.1)$$

It is straightforward to see from the commutator that $|\psi_b\rangle = \hat{\Lambda}|\psi_a\rangle$ either has zero norm or is an eigenstate of \hat{H} with eigenvalue $E_a + \lambda$. Thus if $|\psi_a\rangle$ is the ground state of the system, then $\hat{\Lambda}$ serves as an excitation operator creating an excited state.

Now let us apply this to the case of a large N_c version of the quark-shell model. This model is based on nonrelativistic quark degrees of freedom, and has the standard large N_c scaling rules. The model has rotational and isospin symmetries (with possible small isospin breaking, which we neglect), so that I^2 and J^2 are good quantum numbers of the physical states. In addition, this model in its simplest form has no configuration mixing, so that the number of quarks in a given orbital is also a good quantum number. Our approach is to use excitation operators of the form discussed above on this system, i.e., to find some operator $\hat{\Lambda}$ with the commutator property in Eq. (5.1) that produces excited states when acting on the ground state. However, to leading order in the $1/N_c$ expansion the ground state is highly degenerate (consisting of states with $I=J=1/2, 3/2, \dots$), and thus one can use any superposition of these states as the ground state. Our strategy is to use a hedgehog state as the appropriate superposition. This approach has the advantage of putting the analysis in close parallel to the scattering treatment based on the Skyrme model.

The hedgehog state $|h\rangle$ (which has $K=0$) is given by

$$|h\rangle = \frac{1}{\sqrt{N_c!}} \epsilon_{c_1 c_2 \dots c_{N_c}} \prod_{i=1}^{N_c} a_{h; c_i}^\dagger |0\rangle$$

with

$$a_{h; c}^\dagger \equiv \frac{1}{\sqrt{2}} (a_{1/2, -1/2; c}^\dagger - a_{-1/2, +1/2; c}^\dagger), \quad (5.2)$$

where c represents the quark color and $a_{m_s, m_i; c}^\dagger$ is the creation operator for a quark in the lowest s-wave orbital with spin projection m_s and isospin projection m_i . This state has the (somewhat unfortunate) property that $\langle h | \hat{I}^2 | h \rangle = O(N_c)$. Since excitation energies in the ground-state band are given by $I(I+1)/2\mathcal{I}$, where $\mathcal{I} = \frac{2}{3}(M_\Delta - M_N)^{-1} = O(N_c)$, one sees that the $\langle h | \hat{H} | h \rangle - \langle \text{ground} | \hat{H} | \text{ground} \rangle = O(N_c^0)$. Thus one cannot treat the hedgehog state as degenerate with the ground state at large N_c since the physically interesting quantities—the excitation energies of other bands—are also $O(N_c^0)$. It is simple to finesse this problem: Consider instead eigenstates of the modified Hamiltonian

$$\hat{H}' \equiv \hat{H} - c_2 \hat{I}^2 - c_4 \hat{I}^4 - c_6 \hat{I}^6 - \dots, \quad (5.3)$$

where the coefficients c_2, c_4 , etc. are fixed to ensure that all states in the ground-state band are made degenerate. Note that each eigenstate of \hat{H}' is an eigenstate of \hat{H} with its eigenvalue shifted by $-c_2 \hat{I}^2 - c_4 \hat{I}^4 - c_6 \hat{I}^6 - \dots$. Finding the eigenspectrum of \hat{H}' is therefore equivalent to finding the eigenspectrum of \hat{H} . By construction, $|h\rangle$ is degenerate with the ground state with respect to the operator \hat{H}' .

We first consider the case of a single quark excited above the lowest s-wave orbital. Recall that in the quark-shell model the number of excited quarks is well defined. Now the demonstration that this degeneracy pattern is compatible with the scattering picture consists of two parts. First, we note that if we can show that an operator $\hat{\Lambda}$ satisfying $[\hat{H}', \hat{\Lambda}] = \lambda \hat{\Lambda}$ can be written as a one-body operator that annihilates a ground-state hedgehog quark and creates a quark in an excited orbital with good K (where $\mathbf{K} = \mathbf{I} + \mathbf{J}$), then this operator acting on the state $|h\rangle$ creates an excited eigenstate of the Hamiltonian with well defined K (but generally not of good I or J). Projecting such a state onto states of good I and J then produces a set of degenerate states (mass eigenvalue m_K) of distinct I and J . Moreover, in the large N_c limit the projection onto physical states for this problem is identical to that done in the Skyrme model for scattering states [23]: In that case one finds scattering states with good K on top of the hedgehog and uses a semiclassical projection method with Skyrme wave functions to obtain channels with good I and J . In the present context, the same projection is needed, only now for bound states of fixed K . Since the projections in the two cases are the same, one can reach states of the same quantum numbers in both cases. Thus, without further computation, one sees that degenerate resonances with distinct I and J but labeled by the same intrinsic K in the scattering case in the Skyrme model are mapped one to one onto degenerate bound states in the quark-shell model. Note moreover that, as discussed in Ref. [23], the relations of scattering amplitudes in the Skyrme model are in fact exact large N_c results, and thus we see that the degeneracy patterns

in large N_c scattering are also seen in single-quark excitations in the large N_c quark model.

Before proceeding, it is useful to make a technical remark about the projection. In the case of the Skyrmion, a semiclassical projection was used. In the present context, there is an explicit many-body wave function, for which the standard Peierls-Yoccoz-type projection [28] familiar from many-body theory is applicable. At finite N_c , the two types of projection may differ. However, in the large N_c limit, the relevant overlap functions become narrow and the results of explicit projection agree with the semiclassical result. The key to this result is that the overlap of a (full baryonic) hedgehog with a rotated hedgehog goes like the overlap of single-quark hedgehogs to the n th power, where n is the number of quarks in the hedgehog configuration. Since the single-quark overlap always has a norm of less than or equal to unity and $n \sim N_c$, one sees that as $N_c \rightarrow \infty$ the overlap approaches zero unless the two hedgehogs are aligned. This yields narrow overlap functions and implies the validity of the semiclassical approximation.

Now to complete this argument, we need to prove the claim that the excitation operator $\hat{\Lambda}$ satisfying $[\hat{H}', \hat{\Lambda}] = \lambda \hat{\Lambda}$ can, in fact, be written as a one-body operator that annihilates a ground-state hedgehog quark and creates quark in an excited orbital with good K , and that all excitations with a single quark in an excited orbital can be projected from operators of this general form. To do this, consider the form of the leading-order Hamiltonian (or more precisely \hat{H}') from the quark-shell model. From Refs. [8,9] we know that the leading-order operators that can contribute to single-quark excitations are of the form of $\mathbb{1}, \ell \cdot \mathbf{s}$, and $\ell_{ij}^{(2)} g^{ia} G_c^{ja}/N_c$, where s^i is the matrix element of $\frac{1}{2} \sigma^i$ for the excited quark and ℓ is its orbital excitation, $\ell_{ij}^{(2)} \equiv \frac{1}{2} \{\ell^i, \ell^j\} - \frac{1}{3} \delta^{ij} \ell^2$ is the traceless, symmetric tensor obtained solely from the orbital part of the excited quark (by construction it is a rank-2 spherical tensor under rotations), g^{ia} is the matrix element of $\frac{1}{2} \sigma^i \otimes \frac{1}{2} \tau^a$ for the excited quark, and G_c^{ia} is the matrix element of $\frac{1}{2} \sigma^i \otimes \frac{1}{2} \tau^a$ summed over all of the “core” quarks in the lowest orbital. In these expressions repeated indices are implicitly summed. Note that these are one- and two-body operators. All higher-body operators with $O(N_c^0)$ matrix elements reduce to these forms using the reduction rules of Refs. [8,9,11]. The operators $\mathbb{1}$ and $\ell \cdot \mathbf{s}$ clearly do not depend on the state of the core, nor do they change the K value of the excited quark since both $\mathbb{1}$ and $\ell \cdot \mathbf{s}$ commute with $\mathbf{j} = \ell + \mathbf{s}$. The only one of these operators that mixes core and excited quarks is $\ell_{ij}^{(2)} g^{ia} G_c^{ja}/N_c$. To proceed further we must analyze the effect of this operator in some detail.

The operator $\ell_{ij}^{(2)} g^{ia} G_c^{ja}/N_c$ acts on both the excited quark and the core. It is useful to express each component in terms of pieces that transform under irreducible representations of K . Accordingly, we write

$$\ell_{ij}^{(2)} g^{ia} G_c^{ja} = e^{(0)} G^{(0)} + e_{ia}^{(1,2)} G_{ia}^{(1,2)},$$

where

$$e^{(0)} \equiv \ell_{ia}^{(2)} g^{ia},$$

$$G^{(0)} \equiv \frac{1}{3} G_c^{aa},$$

$$e_{ia}^{(1,2)} \equiv \ell_{ij}^{(2)} g^{ja} - \frac{1}{3} \delta_{ia} e^{(0)},$$

$$G_{ia}^{(1,2)} \equiv G_c^{ia} - \delta_{ia} G^{(0)}, \quad (5.4)$$

and the superscripts (0) and (1,2) refer to the irreducible spherical tensor structure under $\mathbf{K} = \mathbf{I} + \mathbf{J}$. This decomposition is useful for acting upon the class of states in which all of the quarks in the core are in a hedgehog configuration. Suppose one has a state $|\psi\rangle$ in this class. Writing components of G in terms of ladder operators, it is straightforward to see that

$$\frac{1}{N_c} G^{(0)} |\psi\rangle = -\frac{1}{4} \frac{n_{\text{core}}}{N_c} |\psi\rangle, \quad \frac{1}{N_c} G_{ia}^{(1,2)} |\psi\rangle = O(n_{\text{core}}^{1/2}/N_c), \quad (5.5)$$

where n_{core} is the number of quarks in the core; for the case of a single excited quark $n_{\text{core}} = N_c - 1$. Thus, operating on a state of this form it is apparent that

$$\frac{1}{N_c} \ell_{ij}^{(2)} g^{ia} G_c^{ja} |\psi\rangle = -\frac{1}{4} \frac{N_c - 1}{N_c} e^{(0)} |\psi\rangle + O(N_c^{-1/2}). \quad (5.6)$$

We see that *all* of the leading-order operators in the $1/N_c$ expansion acting upon states in the class $|\psi\rangle$ are $K=0$ operators acting on the excited quark or core. This essentially completes the demonstration since it implies that there are eigenstates of \hat{H}' with single-quark excitations of good K acting above a core with all states in the hedgehog; one-body $\hat{\Lambda}$ transition operators that destroy a core hedgehog quark and create an excited quark of fixed K [i.e., of the form $\hat{\Lambda} \propto a_{\text{exc}}^\dagger (\Delta K=0) a_{\text{core}} (\Delta K=0)$] satisfy Eq. (5.1). While the preceding argument was given explicitly for the case of a single quark excited outside the core, it is apparent that an analogous argument holds generally for excitations with $O(N_c^0)$ excited quarks outside the core.

Finally, we note that the hedgehog picture provides a very simple physical interpretation of the various spin-flavor symmetries (S, MS, A). Again, for simplicity consider first the case of a single quark outside a core composed entirely of quarks in a spin-flavor hedgehog. As noted above, these excitations can be labeled by the grand spin K of the excited quark with $\mathbf{K}_{\text{exc}} = \mathbf{I}_{\text{exc}} + \mathbf{J}_{\text{exc}}$. Of course, \mathbf{J}_{exc} has both a spin part and an orbital part. It is useful to decompose \mathbf{K}_{exc} in the following way: $\mathbf{K}_{\text{exc}} = \ell + \mathbf{k}$ where $\mathbf{k} = \mathbf{I}_{\text{exc}} + \mathbf{s}$ is purely a spin-flavor construction independent of the orbital angular momentum. It is clear that k can be either 0 or 1, which together saturate the four possible spin-flavor states of the excited quark. A $k=0$ quark is in a spin-flavor hedgehog, while a $k=1$ quark is orthogonal to the hedgehog. It is trivial to see that a state consisting of a single excited quark in the

$k=0$ (hedgehog configuration) above the hedgehog core must be purely symmetric under spin-flavor since all the quarks are in an identical spin-flavor state (although radial excitations may be present). Next consider a state corresponding to a single $k=1$ quark outside the hedgehog core; since the core alone has $K_{\text{core}}=0$, we may denote such a state combined with the core as $|k=1\rangle$ (noting that the full K of the state still requires the inclusion of orbital angular momentum ℓ). It is straightforward to decompose this state into a symmetric and a mixed-symmetric piece:

$$|k=1\rangle = \sqrt{\frac{1}{N_c}}|k=1\rangle_S + \sqrt{\frac{N_c-1}{N_c}}|k=1\rangle_{\text{MS}}. \quad (5.7)$$

Note that in the large N_c limit such a state becomes purely MS. Thus for large N_c the following interpretation of the symmetry emerges: The S states are those that may be projected from states with a $k=0$ (hedgehog) quark outside the core, while the MS states are those that may be projected from states with a $k=1$ quark outside the core. A similar analysis can be extended to cases with more than one quark outside the core. For example, the A symmetry arises from two non-hedgehog quarks (antisymmetrized with respect to each other in spin-flavor) outside a hedgehog core.

The patterns seen in Table I may be simply understood in terms of this picture. Since the symmetric configurations have $k=0$, one sees immediately that $K=\ell$, and the symmetric representations are precisely those one obtains by adding ℓ to the $I=J$ states in a hedgehog. The MS states are obtained by combining the $|k=1\rangle$ state with ℓ , giving total K values that satisfy $\delta(K\ell 1)$. Similarly, it is easy to understand the fact that the MS and A configurations have the same spectrum of nonstrange states for large N_c . The reason is simply that A is obtained by adding two antisymmetric $k=1$ quarks outside the hedgehog core. However, the antisymmetric combination of two $k=1$ states has a net k of unity since the symmetric combination must yield $k=0$ and $k=2$. Since only the overall k of the quarks outside the core matters, A and MS look the same.

B. Group-theoretical demonstration

Now let us turn to the more formal group-theoretical treatment. The strategy here is to enumerate explicitly the particular representations seen in both the scattering picture and in the quark-shell model and to show explicitly that they are compatible. To proceed, we first note that the angular momentum quantum number L is integral, as are the spin and isospin of the (bosonic) π and η mesons. On the other hand, the baryons involved in the scattering are of course fermionic, and therefore R and hence I and J are half-integral, while K is integral. This is significant because we use that R , I , and J are nonzero.

We now return to the scattering-picture constraints, Eqs. (2.1), that refer to π and η scattering. Note that the $6j$ symbols of Eq. (2.1)—considering only quantum numbers of the initial state—imply the four triangle rules $\delta(LRJ)$, $\delta(R1I)$, $\delta(L1K)$, and $\delta(IJK)$. First we ask whether amplitudes for η scattering can ever possess quantum numbers violating

any of these triangle rules. The constraints in the second of Eqs. (2.1) consist of $\delta(LRJ)$, but also $I=R$ (because the η carries zero isospin) and $K=L$. Now, $I=R$ always satisfies $\delta(R1I)$ because $R\neq 0$. On the other hand, $K=L$ always satisfies $\delta(L1K)$ unless $K=L=0$. It follows that η -baryon scattering allows different amplitudes than in π -baryon scattering only if $K=L=0$, $I=R$, and hence [because of $\delta(LRJ)$], $I=J$. On the other hand, it is clear that π -baryon scattering allows many amplitudes with quantum numbers not allowed in η scattering.

Now, given the I, J quantum numbers of a scattering channel, what values of K appear? From Tables II and III, it is clear for all channels considered that the full set $\delta(IJK)$, $|I-J|\leq K\leq I+J$, appears. However, Eqs. (2.1) give additional constraints on K that must be taken into account: One must check that values for R and L exist [satisfying $\delta(LRJ)$, $\delta(R1I)$, and $\delta(L1K)$ for the π case, or $I=R$ and $K=L$ for the η case] that allow the full range of K for arbitrary half-integral I and J . P conservation places no constraints on the group theory except that it must be conserved throughout any process, and $P=(-1)^{L+1}$ for the resonant state since the scattered meson is pseudoscalar; therefore, we wish to prove the parity blindness of the scattering picture by showing that there exist an even and an odd value of L both satisfying the above constraints.

Consider the value $R=I$, which always satisfies $\delta(R1I)$ since $I\neq 0$. Further, let $L=K$, which always satisfies $\delta(L1K)$ unless $K=0$ (a case we handle in a moment). Then the final $6j$ symbol $\delta(LRJ)$ becomes the same as $\delta(KIJ)$, which is satisfied by assumption. This means that a scattering amplitude of any I, J contains a π scattering amplitude s_{KLL}^π , where K is any nonzero value satisfying $\delta(IJK)$, for which the scattered baryon has $R=I$ and for which $L=K$. Further, $\delta(L1K)$ for $K\neq 0$ is satisfied by three consecutive values of L , namely, $K-1$, K , and $K+1$. Since R and J are nonzero, at least two consecutive values of L satisfy $\delta(LRJ)$, one of which, we have seen, is $L=K$. Thus, for $K\neq 0$, this proves that at least two consecutive values of L satisfy all constraints, allowing both parities [29]. As for $K=0$, the π scattering constraint $\delta(L1K)$ is satisfied solely by $L=1$, while the η scattering constraint δ_{KL} is satisfied solely by $L=0$, giving the required two consecutive values of L satisfying all constraints. We conclude that *a scattering amplitude with any choice of I, J, P contains a reduced amplitude with every value K that satisfies $\delta(IJK)$.*

Now consider the spin-flavor multiplets S, MS, and A discussed in the previous two sections, and in particular the nonstrange N and Δ multiplets listed in Table I. We begin with the S multiplet, anticipating that the proof for MS and A requires little additional effort. The S multiplet for $\ell=0$ consists of states with $I=S$, where S again is the total quark spin, and thus the total baryon spin is given by values allowed by $\mathbf{J}=\mathbf{S}+\boldsymbol{\ell}$, which of course imposes the triangle rule $\delta(IJ\ell)$. Any such triad of values I, J, ℓ (plus P) gives a unique state in a particular S multiplet, as may be seen from the decomposition of S in Eq. (3.1) and the nondegeneracy of resultant multiplet quantum numbers under angular momentum addition. The claim of compatibility of the two pic-

tures for the S multiplet consists of the following necessary and sufficient conditions:

(1) If a state with given values of I, J, P appears in an S multiplet with a given allowed value of ℓ , then the scattering amplitude with I, J, P quantum numbers contains a reduced amplitude with $K = \ell$.

(2) If a scattering amplitude with given values of I, J, P contains an amplitude with a particular allowed value of K , then a state with these quantum numbers appears in an S multiplet with $\ell = K$.

The first statement is proved simply by noting that every value of ℓ satisfying $\delta(IJ\ell)$ gives precisely one state appearing in a particular S multiplet for each value of P , while we have just proved that each value of K satisfying $\delta(IJK)$ (including $K = \ell$) appears in an amplitude with the given I, J, P quantum numbers for at least one π or η scattering process.

The second statement is proved by noting that an amplitude with a given value of K occurs if it satisfies $\delta(IJK)$, regardless of P . Letting $K = \ell$, we see that $\delta(IJ\ell)$ is also satisfied. Including P , this specifies (as we have seen) a unique state in an S multiplet. The proof for S multiplets is thus complete.

Now we return to the MS and A multiplets. Our task is simplified by the fact that we are interested only in N and Δ states, which appear (Table I) with precisely the same multiplicities in these two representations. Moreover, we have seen [Eq. (3.7)] that MS or A multiplets with given ℓ contain the same N and Δ multiplets as given by an effective collection of S multiplets, with values ℓ_{eff} being all those that satisfy $\delta(\ell_{\text{eff}}, \ell, \Delta = 1)$. The proof is thus reduced to one of showing the compatibility between the scattering picture and the quark-shell picture states for a collection of effective S multiplets with ℓ values given by ℓ_{eff} . But this is accomplished simply by recourse to the proof we have just completed: Compatibility is achieved for these effective S multiplets by placing a pole in each amplitude satisfying $K = \ell_{\text{eff}}$. The proof for MS and A multiplets is thus complete.

We arrive at a simple result. Compatibility between the meson-baryon scattering and quark-shell pictures is achieved in the following way: If the orbital excitation of the excited quark in the quark-shell $\text{SU}(4) \times \text{O}(3)$ multiplet is given by ℓ , then for states in S multiplets there exists a scattering partial wave with the quantum numbers of the given state containing a K amplitude with $K = \ell$, and for states in MS or A multiplets there exist scattering amplitudes containing K amplitudes for each value of K satisfying $\delta(K\ell 1)$. Furthermore, reduced amplitudes with these values of K do not appear in scattering amplitudes with quantum numbers corresponding to states not appearing in the given $\text{SU}(4) \times \text{O}(3)$ multiplet. The fact that the masses and widths of resonances may be labeled by K and correspond to poles in the K amplitudes completes the demonstration of compatibility.

It is especially interesting to note that full compatibility would not occur without the possibility of resonance creation both via scattering with π 's and η 's. On the other hand, while it may be tempting to believe that the required inclusion of the pion is an indication of chiral symmetry, the parity blindness of the group theory implies that using light

positive-parity mesons with $I = 0$ and 1 would have worked just as well.

VI. DISCUSSION

We have compared two popular (and often competing) pictures for baryon resonances in the large N_c limit. Both have physical probative value since both explore different aspects of hadronic physics. On one hand, the quark-shell picture certainly is the most successful model in existence for predicting much of the observed spectrum of baryon states, but there is no known good reason that quarks should play the role of the defining degrees of freedom in the highly confining regime of the hadronic environment. On the other hand, baryon resonances truly are observed as “bumps” (or even more obscure features) in meson-baryon scattering amplitudes, but the scattering picture gives no hints as to which amplitudes should even possess resonances, much less where the pole positions should lie.

The fact that each of the two pictures respects the spin-flavor multiplet structure of the other is certainly good news for phenomenology. It implies the existence of a sensible way to perform the $1/N_c$ expansion for baryon resonances. Namely, these broad states [widths of $\text{O}(N_c^0)$] can be treated in a Hamiltonian formalism, just as was done so successfully for the ground-state band, and this treatment respects the symmetries ($I_t = J_t$) implicit in the states' origins as resonances in scattering amplitudes.

However, we caution the reader that what has been presented here is no more than an existence proof of a unified $1/N_c$ expansion; the full treatment awaits an analysis of allowed $1/N_c$ effects [27].

For example, consider the status of configuration mixing in light of our results. The fact that precisely the same non-strange multiplets arise for MS and A flavor representations in large N_c implies that each of the states in one of these multiplets is, in principle, free to mix with its partner in the other multiplet. Detailed quark models tend to disfavor the appearance of A multiplets, chiefly because they require the excitation of two quarks (see Fig. 1), which is usually suppressed (e.g., in one-gluon exchange models). However, the combinatorics of the $N_c - 2$ core quarks negates this suppression in large N_c . Moreover, if $1/N_c$ effects are properly included, they must eventually be sensitive to the differences between the MS and A multiplets when $N_c \leq 7$.

Configuration mixing need not be limited to entire spin-flavor multiplets. For example, the $K = 2$ pole \tilde{m}_2 appearing in the S multiplet 2^+ is precisely the same one as appearing in the $K = 2$ MS (or A) multiplet 1^+ , 2^+ , or 3^+ . Detailed dynamics may suppress some of these spin-flavor multiplets, but some degree of configuration mixing may still be expected at large N_c , such as between $N_{3/2}(S, 2^+)$ and $N_{3/2}(\text{MS}, 2^+)$. Indeed, such mixing is common even in the $N_c = 3$ quark model [31].

As suggested above, a full phenomenological analysis of the higher baryon multiplets must await an accounting of the $1/N_c$ corrections. From the theoretical side, this is clearly necessary not only because operators corresponding to important physical effects might first arise at $\text{O}(1/N_c)$, but be-

cause the resonance spectrum itself is different for $N_c > 3$, and such states must be consistently decoupled before one has a fully usable formalism for studying the $N_c = 3$ case. From the experimental side, a quick glance at the status of the higher baryon states [32] indicates a number of resonances of dubious existence; assuming the verity of phantom states (or missing relevant states) could easily lead to a false interpretation about which underlying dynamical effects are most important.

In short, the $1/N_c$ expansion for baryon resonances should not be viewed as the final arbiter of competing dynamical

pictures, but rather as a baseline of symmetry constraints, upon which new ideas for dynamics can be studied.

ACKNOWLEDGMENTS

T.D.C. acknowledges the support of the U.S. Department of Energy through grant DE-FG02-93ER-40762. R.F.L. acknowledges support from the National Science Foundation under Grant No. PHY-0140362, and thanks S. Capstick for valuable discussions.

-
- [1] T.D. Cohen and R.F. Lebed, Phys. Rev. Lett. **91**, 012001 (2003); Phys. Rev. D **67**, 096008 (2003).
 - [2] J.-L. Gervais and B. Sakita, Phys. Rev. Lett. **52**, 87 (1984); Phys. Rev. D **30**, 1795 (1984).
 - [3] R.F. Dashen and A.V. Manohar, Phys. Lett. B **315**, 425 (1993); **315**, 438 (1993).
 - [4] E. Jenkins, Phys. Lett. B **315**, 441 (1993).
 - [5] R.F. Dashen, E. Jenkins, and A.V. Manohar, Phys. Rev. D **49**, 4713 (1994).
 - [6] D. Pirjol and T.-M. Yan, Phys. Rev. D **56**, 5483 (1997); **57**, 5434 (1998).
 - [7] D. Pirjol and C. Schat, Phys. Rev. D **67**, 096009 (2003).
 - [8] C.E. Carlson, C.D. Carone, J.L. Goity, and R.F. Lebed, Phys. Lett. B **438**, 327 (1998).
 - [9] C.E. Carlson, C.D. Carone, J.L. Goity, and R.F. Lebed, Phys. Rev. D **59**, 114008 (1999).
 - [10] A.J. Buchmann and R.F. Lebed, Phys. Rev. D **62**, 096005 (2000).
 - [11] R.F. Dashen, E. Jenkins, and A.V. Manohar, Phys. Rev. D **51**, 3697 (1995).
 - [12] E. Jenkins and R.F. Lebed, Phys. Rev. D **52**, 282 (1995).
 - [13] M.A. Luty and J. March-Russell, Nucl. Phys. B **426**, 71 (1994); M.A. Luty, J. March-Russell, and M.J. White, Phys. Rev. D **51**, 2332 (1995).
 - [14] C.D. Carone, H. Georgi, and S. Osofsky, Phys. Lett. B **322**, 227 (1994).
 - [15] A.J. Buchmann, J.A. Hester, and R.F. Lebed, Phys. Rev. D **66**, 056002 (2002).
 - [16] C.D. Carone, H. Georgi, L. Kaplan, and D. Morin, Phys. Rev. D **50**, 5793 (1994).
 - [17] J.L. Goity, Phys. Lett. B **414**, 140 (1997).
 - [18] C.E. Carlson and C.D. Carone, Phys. Lett. B **441**, 363 (1998); Phys. Rev. D **58**, 053005 (1998).
 - [19] C.L. Schat, J.L. Goity, and N.N. Scoccola, Phys. Rev. Lett. **88**, 102002 (2002); J.L. Goity, C.L. Schat, and N.N. Scoccola, Phys. Rev. D **66**, 114014 (2002).
 - [20] C.E. Carlson and C.D. Carone, Phys. Lett. B **484**, 260 (2000).
 - [21] J.L. Goity, C.L. Schat, and N.N. Scoccola, Phys. Lett. B **564**, 83 (2003).
 - [22] A. Hayashi, G. Eckart, G. Holzwarth, and H. Walliser, Phys. Lett. **147B**, 5 (1984).
 - [23] M.P. Mattis and M.E. Peskin, Phys. Rev. D **32**, 58 (1985).
 - [24] M.P. Mattis and M. Mukerjee, Phys. Rev. Lett. **61**, 1344 (1988).
 - [25] M.P. Mattis, Phys. Rev. Lett. **56**, 1103 (1986); Phys. Rev. D **39**, 994 (1989); Phys. Rev. Lett. **63**, 1455 (1989).
 - [26] M.P. Mattis and M. Karliner, Phys. Rev. D **31**, 2833 (1985).
 - [27] T.D. Cohen and R.F. Lebed (unpublished).
 - [28] R.E. Peierls and J. Yoccoz, Proc. Phys. Soc., London, Sect. A **70**, 381 (1957).
 - [29] There is one exception to this proof, which is quite rare, but is dispensed with here for completeness: It is possible for a $6j$ symbol to vanish even if all relevant triangle rules are satisfied. This can happen for the π scattering case with $I=R$, $L=K > 0$ discussed in the text; however, in this case the η amplitude with the same quantum numbers is always allowed [see Eq.(2.1)], and contains the desired amplitude s_K^{η} . The only such “exceptional zero” occurring in this analysis is the case $I=R=3/2$, $L=K=3$, $J=7/2$, the $F_{37}^{\pi\Delta\Delta}$ amplitude for $\Delta_{7/2}$ in Table III, where the $K=3$ amplitude is seen to be absent. Indeed, this is the only such case up to at least $K=50$. The $6j$ symbols corresponding to $L=K\pm 1$ are always nonzero if they satisfy all relevant triangle rules, as can be shown from an explicit expression [30].
 - [30] A.R. Edmonds, *Angular Momentum in Quantum Mechanics* (Princeton University Press, Princeton, NJ, 1996).
 - [31] C.P. Forsyth and R.E. Cutkosky, Z. Phys. C **18**, 219 (1983); S. Capstick and N. Isgur, Phys. Rev. D **34**, 2809 (1986).
 - [32] Particle Data Group, K. Hagiwara *et al.*, Phys. Rev. D **66**, 010001 (2002).